

Maximization of the fundamental frequencies of laminated truncated conical shells with respect to fiber orientations

H.-T. Hu ^{*}, S.-C. Ou

Department of Civil Engineering, National Cheng Kung University, Tainan, 70101 Taiwan, ROC

Abstract

The fundamental frequencies of laminated truncated conical shells with a given material system are maximized with respect to fiber orientations by using a sequential linear programming method with a simple move-limit strategy. The significant influences of shell thickness, shell length, shell radius ratio and cutout on the maximum fundamental frequencies and the associated optimal fiber orientations are demonstrated. © 2001 Elsevier Science Ltd. All rights reserved.

Keywords: Maximization; Fundamental frequency; Truncated conical shells; Sequential linear programming

1. Introduction

Due to light weight and high strength, the use of fiber-reinforced composite laminated materials in aerospace industry have increased rapidly in recent years. The truncated conical shell configuration is widely used in aircraft, spacecraft, rocket and missile, which are frequently subjected to dynamic loads in service. Hence, knowledge of dynamic characteristics of truncated conical shells constructed of fiber-reinforced laminated materials, such as their fundamental frequencies, is essential [1].

The fundamental frequencies of laminated truncated conical shells highly depend on ply orientations, boundary conditions, and geometric variables such as thickness, shell radius ratio, shell length and cutout [2–10]. Therefore, for laminated truncated conical shells with a given material system, geometric shape, thickness and boundary condition, the proper selection of appropriate lamination to maximize the fundamental frequency of the shells becomes an interesting problem [11–13].

Research on the subject of structural optimization has been reported by many investigators [14]. Among various optimization schemes, the method of sequential linear programming has been successfully applied to many large scale structural problems [15,16]. In this

investigation, optimization of fiber-reinforced laminated truncated conical shells to maximize their fundamental frequencies with respect to fiber orientations is performed by using a sequential linear programming method together with a simple move-limit strategy. The fundamental frequencies of laminated truncated conical shells are calculated by using the ABAQUS finite element program [17]. In the paper, the constitutive equations for fiber-composite laminate, vibration analysis and optimization method are briefly reviewed. Then the influence of shell thickness, shell length, shell radius ratio and cutout on the optimal fundamental frequency and the associated optimal fiber orientation of laminated truncated conical shells is presented. Finally, important conclusions obtained from the study are given.

2. Constitutive matrix for fiber-composite laminae

In the finite element analysis, the laminated truncated conical shells are modeled by eight-node isoparametric shell elements with six degrees of freedom per node (three displacements and three rotations). The doubly curved shell element has four edges (three nodes per edge) and can be used to model fairly complicated curved surface structures very accurately. The reduced integration rule together with hourglass stiffness control is employed to formulate the element stiffness matrix [17]. During the analysis, the constitutive matrices of composite materials at element integration points must be calculated before the stiffness matrices are assembled

^{*} Corresponding author. Tel.: +886-6-2757-57 Ext. 63168; fax: +886-6-2358-542.

E-mail address: hthu@mail.ncku.edu.tw (H.-T. Hu).

from element level to global level. For fiber-composite laminated materials, each lamina can be considered as an orthotropic layer in a plane stress condition (Fig. 1). The stress-strain relations for a lamina in the material coordinates (1, 2, 3) at an element integration point can be written as

$$\{\sigma'\} = [Q'_1]\{\varepsilon'\}, \quad \{\tau'\} = [Q'_2]\{\gamma'\}, \quad (1)$$

$$[Q'_1] = \begin{bmatrix} \frac{E_{11}}{1 - \nu_{12}\nu_{21}} & \frac{\nu_{12}E_{22}}{1 - \nu_{12}\nu_{21}} & 0 \\ \frac{\nu_{21}E_{11}}{1 - \nu_{12}\nu_{21}} & \frac{E_{22}}{1 - \nu_{12}\nu_{21}} & 0 \\ 0 & 0 & G_{12} \end{bmatrix}, \quad (2)$$

$$[Q'_2] = \begin{bmatrix} \alpha_1 G_{13} & 0 \\ 0 & \alpha_2 G_{23} \end{bmatrix},$$

where

$$\{\sigma'\} = \{\sigma_1, \sigma_2, \tau_{12}\}^T, \quad \{\tau'\} = \{\tau_{13}, \sigma_{23}\}^T, \\ \{\varepsilon'\} = \{\varepsilon_1, \varepsilon_2, \gamma_{12}\}^T, \quad \{\gamma'\} = \{\gamma_{13}, \gamma_{23}\}^T.$$

The α_1 and α_2 are shear correction factors, which are calculated in ABAQUS by assuming that the transverse shear energy through the thickness of laminate is equal to that in unidirectional bending [17,18]. The constitutive equations for the lamina in the element coordinates (x, y, z) become

$$\{\sigma\} = [Q_1]\{\varepsilon\}, \quad [Q_1] = [T_1]^T [Q'_1] [T_1], \quad (3)$$

$$\{\tau\} = [Q_2]\{\gamma\}, \quad [Q_2] = [T_2]^T [Q'_2] [T_2], \quad (4)$$

$$[T_1] = \begin{bmatrix} \cos^2 \theta & \sin^2 \theta & \sin \theta \cos \theta \\ \sin^2 \theta & \cos^2 \theta & -\sin \theta \cos \theta \\ -2 \sin \theta \cos \theta & 2 \sin \theta \cos \theta & \cos^2 \theta - \sin^2 \theta \end{bmatrix},$$

$$[T_2] = \begin{bmatrix} \cos \theta & \sin \theta \\ -\sin \theta & \cos \theta \end{bmatrix}, \quad (5)$$

where

$$\{\sigma\} = \{\sigma_x, \sigma_y, \tau_{xy}\}^T, \quad \{\tau\} = \{\tau_{xz}, \tau_{yz}\}^T,$$

$$\{\varepsilon\} = \{\varepsilon_x, \varepsilon_y, \gamma_{xy}\}^T, \quad \{\gamma\} = \{\gamma_{xz}, \gamma_{yz}\}^T,$$

and θ is measured counterclockwise about the z -axis from the element local x -axis to the material 1-axis. The element coordinate system (x, y, z) is a curvilinear local system (Fig. 1) that is different from the structural global coordinate (X, Y, Z). While the element x -axis is in the longitudinal direction of the truncated conical shell, element y - and z -axes are in the circumferential and the radial directions of the truncated conical shell. Let $\{\varepsilon_0\} = \{\varepsilon_{x0}, \varepsilon_{y0}, \gamma_{xy0}\}^T$ be the in-plane strains at the mid-surface of the laminate section, $\{\kappa\} = \{\kappa_x, \kappa_y, \kappa_{xy}\}^T$ the curvatures, and h the total thickness of the section. If there are n layers in the layup, the stress resultants, $\{N\} = \{N_x, N_y, N_{xy}\}^T$, $\{M\} = \{M_x, M_y, M_{xy}\}^T$ and $\{V\} = \{V_x, V_y\}^T$, can be defined as

$$\begin{Bmatrix} \{N\} \\ \{M\} \\ \{V\} \end{Bmatrix} = \int_{-h/2}^{h/2} \begin{Bmatrix} \{\sigma\} \\ z\{\sigma\} \\ \{\tau\} \end{Bmatrix} dz \\ = \sum_{j=1}^n \begin{bmatrix} (z_{jt} - z_{jb})[Q_1] & \frac{1}{2}(z_{jt}^2 - z_{jb}^2)[Q_1] & [0] \\ \frac{1}{2}(z_{jt}^2 - z_{jb}^2)[Q_1] & \frac{1}{3}(z_{jt}^3 - z_{jb}^3)[Q_1] & [0] \\ [0]^T & [0]^T & (z_{jt} - z_{jb})[Q_2] \end{bmatrix} \begin{Bmatrix} \{\varepsilon_0\} \\ \{\kappa\} \\ \{\gamma\} \end{Bmatrix}, \quad (6)$$

where z_{jt} and z_{jb} are the distance from the mid-surface of the section to the top and the bottom of the j th layer, respectively. The $[0]$ is a 3 by 2 matrix with all the coefficients equal to zero.

3. Vibration analysis

For the finite-element analysis of an undamped structure, if there are no external forces, the equation of motion of the structure can be written in the following form [19]:

$$[M]\{\ddot{D}\} + [K]\{D\} = \{0\}, \quad (7)$$

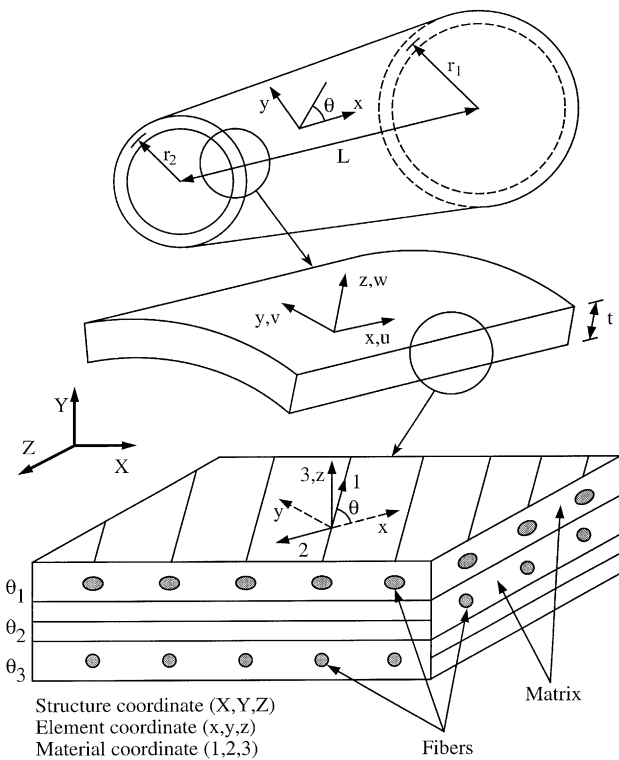


Fig. 1. Material, element and structure coordinates of laminated truncated conical shells.

where $\{D\}$ is a vector containing the unrestrained nodal degrees of freedoms, $[M]$ a structural mass matrix, $[K]$ a structural stiffness matrix, and $\{0\}$ a zero vector. Since $\{D\}$ undergoes harmonic motion, the vectors $\{D\}$ and $\{\ddot{D}\}$ become

$$\{D\} = \{\bar{D}\} \sin \omega t; \quad \{\ddot{D}\} = -\omega^2 \{\bar{D}\} \sin \omega t, \quad (8)$$

where $\{\bar{D}\}$ vector contains the amplitudes of $\{D\}$ vector and ω is the frequency. Then Eq. (7) can be written in an eigenvalue expression as

$$([K] - \lambda[M])\{\bar{D}\} = \{0\}, \quad (9)$$

where $\lambda = \omega^2$ is the eigenvalue and $\{\bar{D}\}$ becomes the eigenvector. In ABAQUS, a subspace iteration procedure [20] is used to solve for the eigenvalues, the natural frequency, and the eigenvectors. The obtained smallest natural frequency (fundamental frequency) is then the objective function for maximization.

4. Sequential linear programming

A general optimization problem may be defined as the following:

$$\text{Maximize } f(\underline{x}) \quad (10a)$$

$$\text{subject to } g_i(\underline{x}) \leq 0, \quad i = 1, \dots, r, \quad (10b)$$

$$h_j(\underline{x}) = 0, \quad j = r + 1, \dots, m, \quad (10c)$$

$$p_k \leq x_k \leq q_k, \quad k = 1, \dots, n, \quad (10d)$$

where $f(\underline{x})$ is an objective function, $g_i(\underline{x})$ are inequality constraints, $h_j(\underline{x})$ are equality constraints, and $\underline{x} = \{x_1, x_2, \dots, x_n\}^T$ is a vector of design variables.

For the general optimization problem of Eqs. (10a)–(10d), a linearized problem may be constructed by approximating the nonlinear functions about a current solution point, $\underline{x}_0 = \{x_{01}, x_{02}, \dots, x_{0n}\}^T$, in a first-order Taylor series expansion as follows:

$$\text{Maximize } f(\underline{x}) = f(\underline{x}_0) + \nabla f(\underline{x}_0)^T \delta \underline{x} \quad (11a)$$

$$\text{subject to } g_i(\underline{x}) = g_i(\underline{x}_0) + \nabla g_i(\underline{x}_0)^T \delta \underline{x} \leq 0, \quad i = 1, \dots, r, \quad (11b)$$

$$h_j(\underline{x}) = h_j(\underline{x}_0) + \nabla h_j(\underline{x}_0)^T \delta \underline{x} = 0, \quad j = r + 1, \dots, m, \quad (11c)$$

$$p_k \leq x_k \leq q_k, \quad k = 1, \dots, n, \quad (11d)$$

where $\delta \underline{x} = \{x_1 - x_{01}, x_2 - x_{02}, \dots, x_n - x_{0n}\}^T$. It is clear that Eqs. (11a)–(11d) represent a linear programming problem where variables are contained in the vector $\delta \underline{x}$. A solution for Eqs. (11a)–(11d) may be easily obtained by the simplex method [21]. After obtaining a solution of Eqs. (11a)–(11d), say \underline{x}_1 , we can linearize the original problem, Eqs. (10a)–(10d), at \underline{x}_1 and solve the new linear programming problem. The process is repeated until a

precise solution is achieved. This approach is referred to as sequential linear programming [15,16].

Although the procedure for a sequential linear programming is simple, difficulties may arise during the iterations. First, the optimum solution for the approximate linear problem may violate the constraint conditions of the original optimization problem. Second, in a nonlinear problem, the true optimum solution may appear between two constraint intersections. A straightforward successive linearization may lead to an oscillation of the solution between the widely separated values. Difficulties in dealing with such a problem may be avoided by imposing a “move limit” on the linear approximation [15,16]. The concept of a move limit is that a set of box-like admissible constraints are placed in the range of $\delta \underline{x}$ and it should gradually approach zero as the iterative process continues. It is known that computational economy and accuracy of the approximate solution may depend greatly on the choice of the move limit. In general, the choice of a suitable move limit depends on experience and also on the results of previous steps.

The algorithm of the sequential linear programming with selected move limits may be summarized as follows:

(1) Linearize the nonlinear objective function and associated constraints with respect to an initial guess \underline{x}_0 .

(2) Impose move limits in the form of $-\underline{S} \leq (\underline{x} - \underline{x}_0) \leq \underline{R}$, where \underline{S} and \underline{R} are properly chosen lower and upper bounds.

(3) Solve the approximate linear programming problem to obtain an optimum solution \underline{x}_1 .

(4) Repeat the procedures from (1) to (3) by redefining \underline{x}_1 with \underline{x}_0 until either the subsequent solutions do not change significantly (i.e., true convergence) or the move limit approaches zero (i.e., forced convergence).

If the solution obtained is due to forced convergence, the procedures from (1) to (4) should be repeated with another initial guess.

5. Numerical analysis

5.1. Laminated truncated conical shells with various lengths, radius ratios and boundary conditions

In this section laminated truncated conical shells with four types of boundary conditions (Fig. 2(a)) are considered, which are two ends fixed (denoted by FF), left end simply supported and right end fixed (denoted by SF), left end fixed and right end simply supported (denoted by FS), and two ends simply supported (denoted by SS). The radius of the truncated conical shell at the right edge, r_1 , is equal to 10 cm and the radius of the shell at the left edge, r_2 , is selected to be 6, 8, and 10 cm (radius ratio $r_2/r_1 = 0.6, 0.8$ and 1). The length of shell L varies between 10 and 40 cm. The laminate layups of

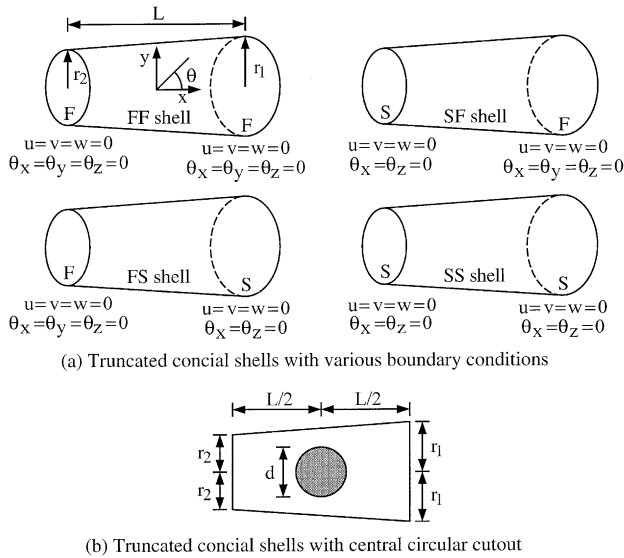


Fig. 2. Boundary condition and geometry of laminated truncated conical shells.

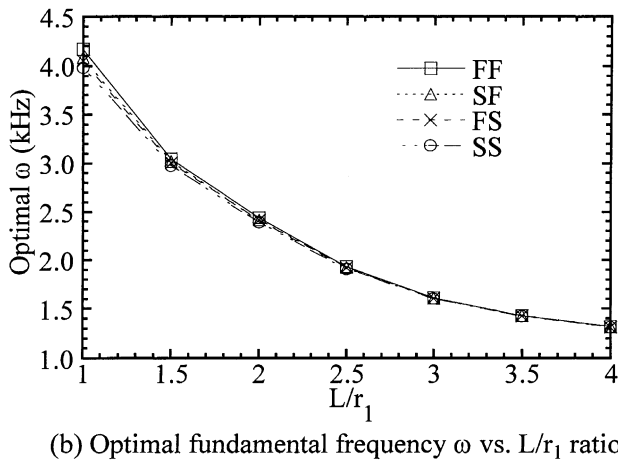
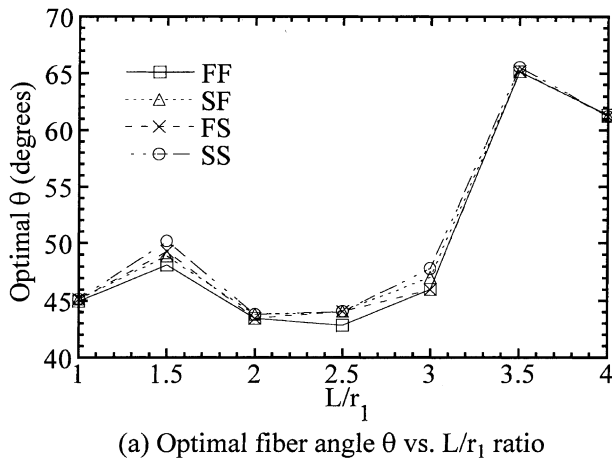


Fig. 3. Effect of boundary conditions and L/r_1 ratio on optimal fiber angle and optimal fundamental frequency of $[\pm\theta/90_2/0]_{2s}$ laminated truncated conical shells ($r_1 = 10$ cm, $r_2 = 6$ cm).

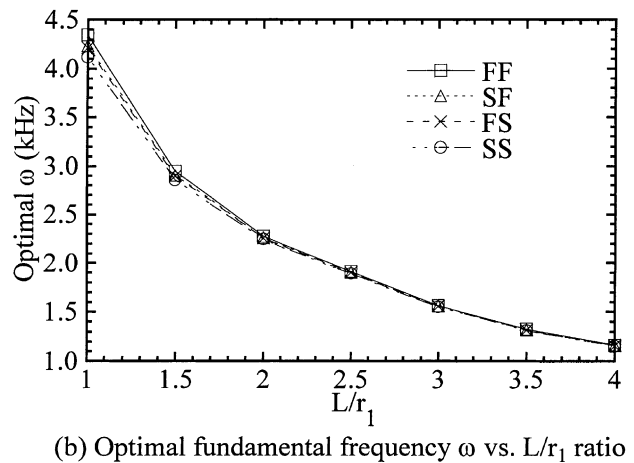
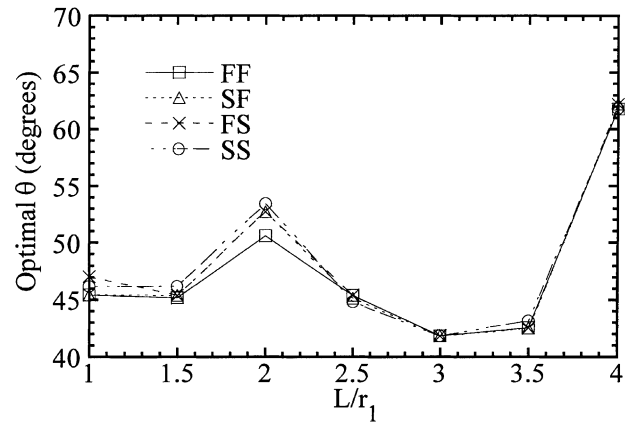
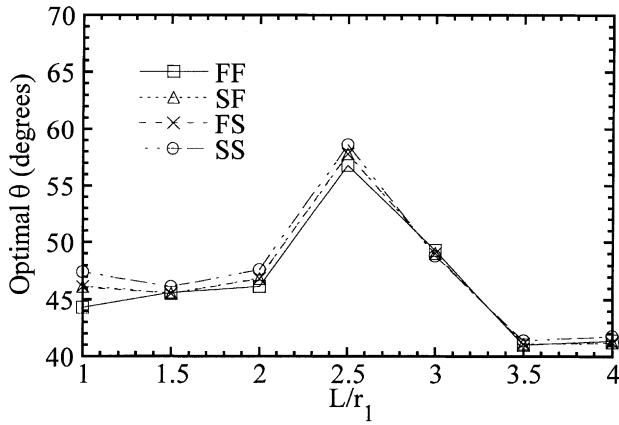


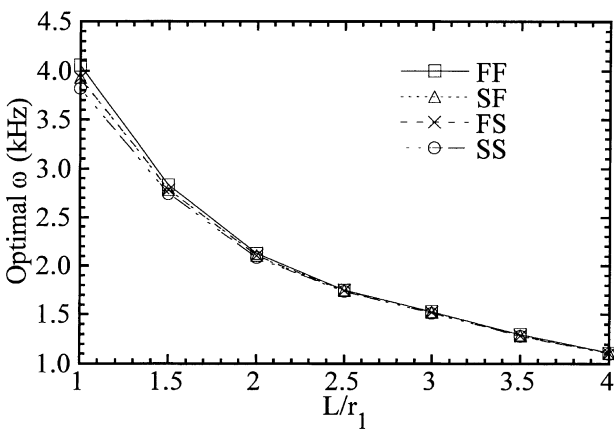
Fig. 4. Effect of boundary conditions and L/r_1 ratio on optimal fiber angle and optimal fundamental frequency of $[\pm\theta/90_2/0]_{2s}$ laminated truncated conical shells ($r_1 = 10$ cm, $r_2 = 8$ cm).

the shells are $[\pm\theta/90_2/0]_{ns}$ and the thickness of each ply is 0.125 mm. In order to study the influence of shell thickness on the results of optimization, $n = 2$ (20-ply thin shell) and 10 (100-ply thick shell) are selected for analysis. The lamina consists of Graphite/Epoxy and material constitutive properties are taken from Crawley [22], which are $E_{11} = 128$ GPa, $E_{22} = 11$ GPa, $\nu_{12} = 0.25$, $G_{12} = G_{13} = 4.48$ GPa, $G_{23} = 1.53$ GPa, $\rho = 1.5 \times 10^3$ kg/m³. In the analysis, no symmetry simplifications are made for those shells. Based on the convergent studies of the laminated truncated conical shells [23], it was decided to use 64 shell elements (16 rows in circumferential direction and four rows in longitudinal direction) to model the truncated conical shells with $L/r_1 = 1$ and 208 shell elements (16 rows in circumferential direction and 13 rows in longitudinal direction) to model the shells with $L/r_1 = 4$. For shells with $1 < L/r_1 < 4$, the numbers of elements are properly scaled between 64 and 208.

Based on the sequential linear programming method, in each iteration the current linearized optimization problem becomes:



(a) Optimal fiber angle θ vs. L/r_1 ratio



(b) Optimal fundamental frequency ω vs. L/r_1 ratio

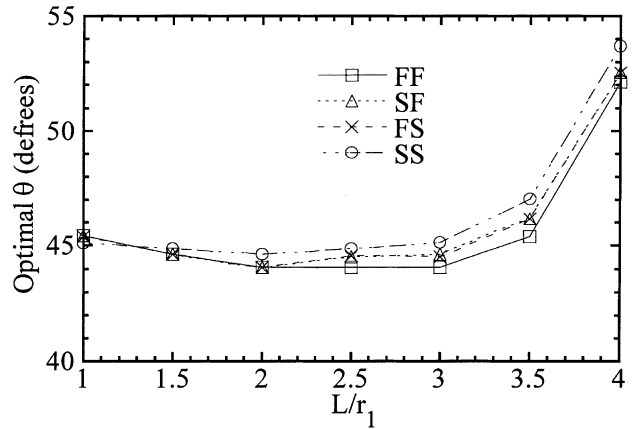
Fig. 5. Effect of boundary conditions and L/r_1 ratio on optimal fiber angle and optimal fundamental frequency of $[\pm\theta/90_2/0]_{2s}$ laminated truncated conical shells ($r_1 = 10$ cm, $r_2 = 10$ cm).

$$\text{Maximize } \omega(\theta) = \omega(\theta_0) + (\theta - \theta_0) \left. \frac{\partial \omega}{\partial \theta} \right|_{\theta=\theta_0} \quad (12a)$$

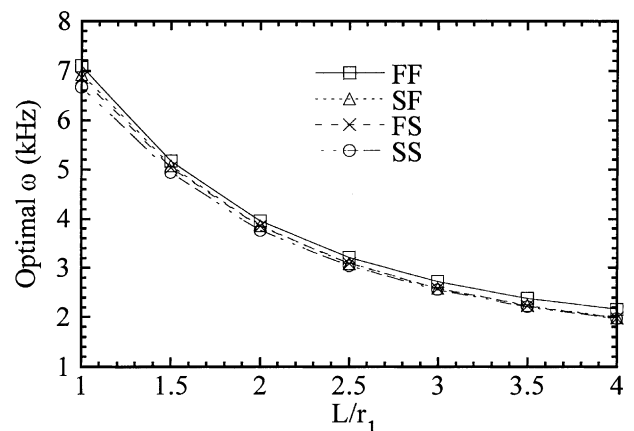
$$\text{subject to } 0^\circ \leq \theta \leq 90^\circ, \quad (12b)$$

$$-r \times q \times 0.5^\circ \leq (\theta - \theta_0) \leq r \times q \times 0.5^\circ, \quad (12c)$$

where ω is the fundamental frequency. The θ_0 is a solution obtained in the previous iteration. The r and q in Eq. (12c) are the size and the reduction rate of the move limit. Based on past experience [24,25], the values of r and q are selected to be 10° and $0.9^{(N-1)}$ in the present study, where N is a current iteration number. In order to control the oscillation of the solution, a parameter 0.5^s is introduced in the move limit, where s is the number of oscillations of the derivative $\partial\omega/\partial\theta$ that has taken place before the current iteration. The value of s increases by 1 if the sign of $\partial\omega/\partial\theta$ changes. Whenever oscillation of the solution occurs, the range of the move limit is reduced to half of its current value. This expedites the solution convergence rate very rapidly.



(a) Optimal fiber angle θ vs. L/r_1 ratio



(b) Optimal fundamental frequency ω vs. L/r_1 ratio

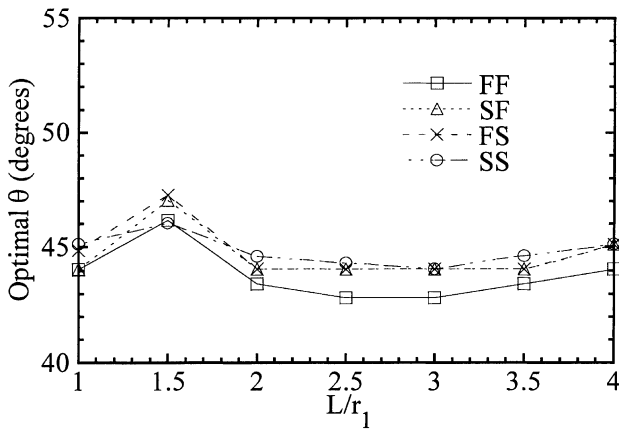
Fig. 6. Effect of boundary conditions and L/r_1 ratio on optimal fiber angle and optimal fundamental frequency of $[\pm\theta/90_2/0]_{10s}$ laminated truncated conical shells ($r_1 = 10$ cm, $r_2 = 6$ cm).

The $\partial\omega/\partial\theta$ term in Eq. (12a) may be approximated by using a forward finite-difference method with the following form:

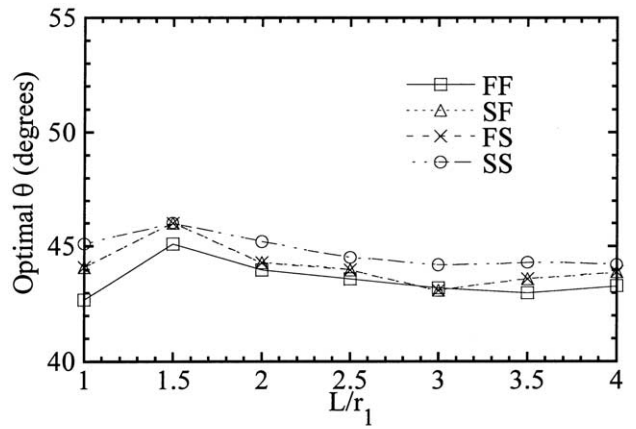
$$\frac{\partial \omega}{\partial \theta} = \frac{[\omega(\theta_0 + \Delta\theta) - \omega(\theta_0)]}{\Delta\theta} \quad (13)$$

Hence, in order to determine the value of $\partial\omega/\partial\theta$ numerically, two finite element analyses to compute $\omega(\theta_0)$ and $\omega(\theta_0 + \Delta\theta)$ are needed in each iteration. In this study, the value of $\Delta\theta$ is selected to be 1° in most iterations.

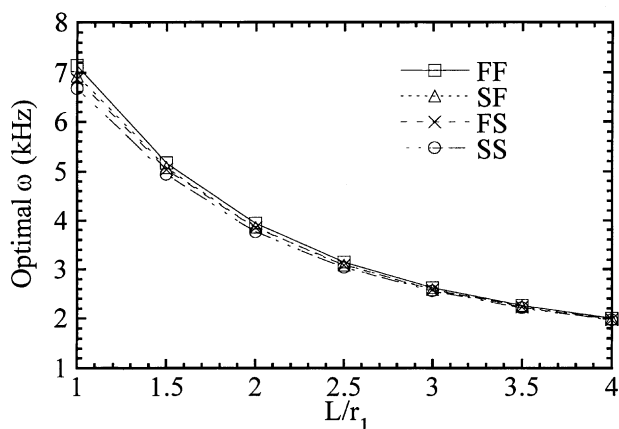
Fig. 3 shows the optimal fiber angle θ and the associated optimal fundamental frequency ω with respect to the L/r_1 ratio for thin $[\pm\theta/90_2/0]_{2s}$ laminated truncated conical shells with various edge conditions and with $r_2/r_1 = 0.6$. From Fig. 3(a) we can see that the optimal fiber angles θ of the laminated truncated conical shells seem not to be sensitive to the boundary conditions. In addition, the optimal fiber angles θ seem to be fourth-order polynomials of L/r_1 ratio. Under the same L/r_1 ratio, the SS shells usually have the largest values



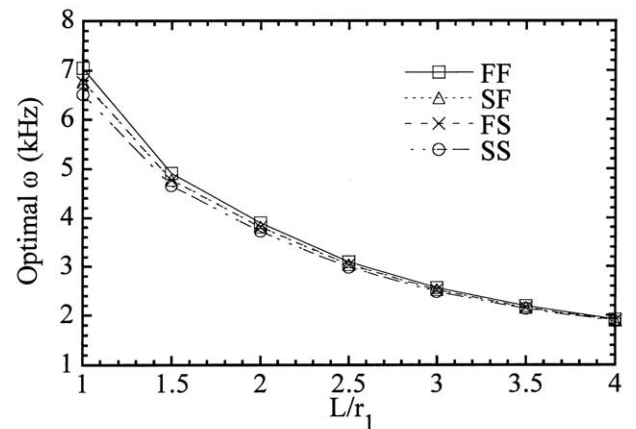
(a) Optimal fiber angle θ vs. L/r_1 ratio



(a) Optimal fiber angle θ vs. L/r_1 ratio



(b) Optimal fundamental frequency ω vs. L/r_1 ratio



(b) Optimal fundamental frequency ω vs. L/r_1 ratio

Fig. 7. Effect of boundary conditions and L/r_1 ratio on optimal fiber angle and optimal fundamental frequency of $[\pm\theta/90_2/0]_{10s}$ laminated truncated conical shells ($r_1 = 10$ cm, $r_2 = 8$ cm).

Fig. 8. Effect of boundary conditions and L/r_1 ratio on optimal fiber angle and optimal fundamental frequency of $[\pm\theta/90_2/0]_{10s}$ laminated truncated conical shells ($r_1 = 10$ cm, $r_2 = 10$ cm).

for the optimal fiber angles and the FF shells usually have the smallest values for the optimal fiber angles. From Fig. 3(b), we can observe that the optimal fundamental frequency ω generally decreases with the increasing of L/r_1 ratio and that the optimal fundamental frequency ω is also insensitive to the boundary conditions. Nevertheless, among these shells under the same geometric configuration, the FF shells have the highest optimal fundamental frequencies, and the SS panels have the lowest optimal fundamental frequencies. Although, the optimal fundamental frequencies ω for the SF shells are slightly higher than those of the FS shells, their differences are hard to distinguish. This is because the influence of boundary conditions are small. Figs. 4 and 5 show the optimal fiber angle θ and the associated optimal fundamental frequency ω with respect to the L/r_1 ratio for thin ($[\pm\theta/90_2/0]_{2s}$) laminated truncated conical shells with various edge conditions and with r_2/r_1 equal to 0.8 and 1, respectively. Comparing Fig. 4(a) and 5(a) with Fig. 3(a), we can find that the curves of the optimal fiber angle θ of the laminated truncated

conical shells seem to “shift” toward the right direction. For example, the local maximum point at $L/r_1 = 1.5$ in Fig. 3(a) shifts to the local maximum point at $L/r_1 = 2$ in Fig. 4(a) and to the global maximum point at $L/r_1 = 2.5$ in Fig. 5(a). The peak values of the optimal fiber angle at the aforementioned local maximum/global maximum points increase when the r_2/r_1 ratio increases. In addition, the range of the optimal fiber angle decreases with the increasing of the r_2/r_1 ratio. For example, $43^\circ \leq \theta \leq 66^\circ$ when $r_2/r_1 = 0.6$, $42^\circ \leq \theta \leq 62^\circ$ when $r_2/r_1 = 0.8$, and, $41^\circ \leq \theta \leq 59^\circ$ when $r_2/r_1 = 1$. Fig. 4(b) and 5(b) show similar trend as Fig. 3(b) and it seems that the optimal fundamental frequency ω is not influenced by the r_2/r_1 ratio significantly.

Figs. 6–8 show the optimal fiber angle θ and the associated optimal fundamental frequency ω with respect to the L/r_1 ratio for thick ($[\pm\theta/90_2/0]_{10s}$) laminated truncated conical shells with various edge conditions and with r_2/r_1 equal to 0.6, 0.8 and 1, respectively. From Fig. 6(a) we can see that the optimal fiber angles θ of the laminated truncated conical shells seem to be second-

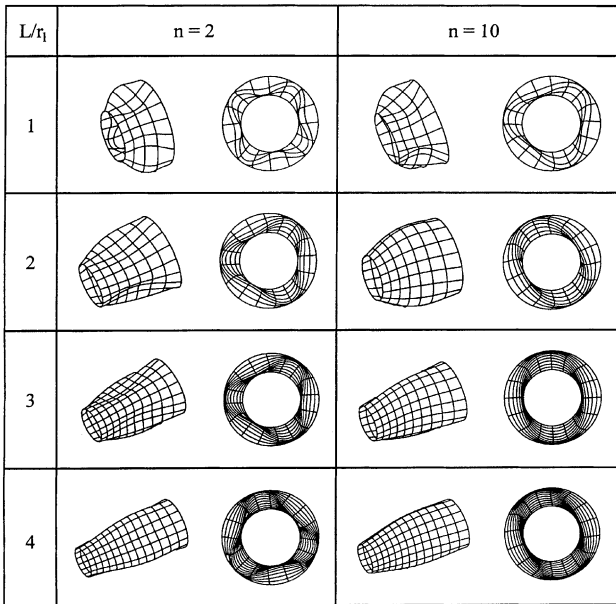


Fig. 9. Fundamental vibration modes of $[\pm\theta/90_2/0]_{ms}$ laminated truncated conical shells with two fixed ends and under optimal fiber angles ($r_1 = 10$ cm, $r_2 = 6$ cm).

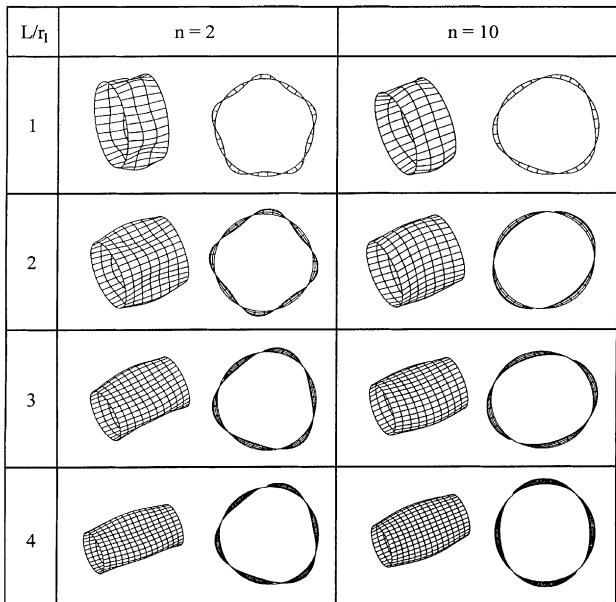
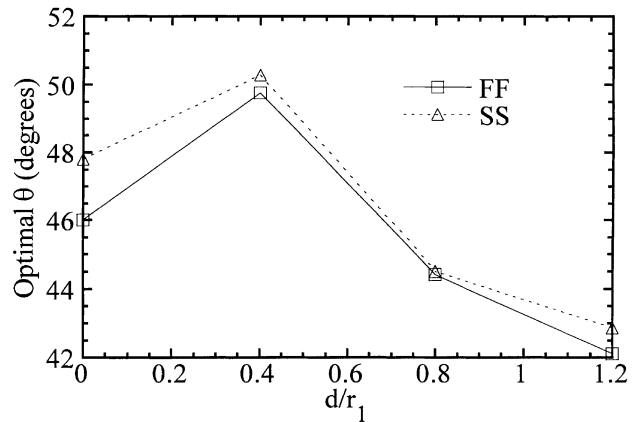
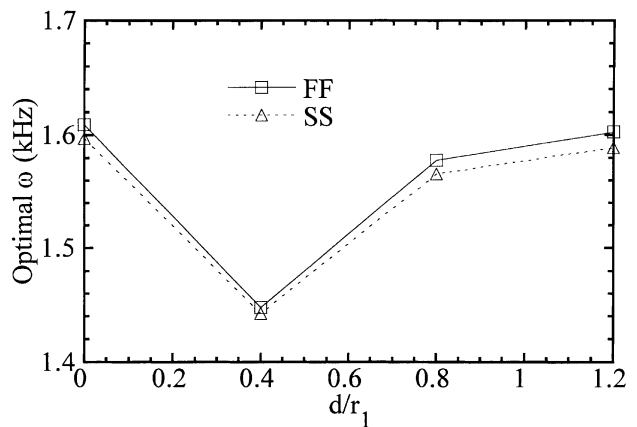


Fig. 10. Fundamental vibration modes of $[\pm\theta/90_2/0]_{ms}$ laminated truncated conical shells with two fixed ends and under optimal fiber angles ($r_1 = 10$ cm, $r_2 = 10$ cm).

order polynomials of L/r_1 ratio. From Figs. 7(a) and 8(a), we can observe that the curves of the optimal fiber angle have maximum points at $L/r_1 = 1.5$. Again, the range of the optimal fiber angle θ decreases with the increasing of the r_2/r_1 ratio. Comparing Figs. 6–8(a) with Figs. 3–5(a), it can be seen that the shell thickness



(a) Optimal fiber angle θ vs. d/r_1 ratio



(b) Optimal fundamental frequency ω vs. d/r_1 ratio

Fig. 11. Effect of boundary conditions and d/r_1 ratio on optimal fiber angle and optimal fundamental frequency of $[\pm\theta/90_2/0]_{2s}$ laminated truncated conical shells with central circular cutouts ($r_1 = 10$ cm, $r_2 = 6$ cm, $L = 30$ cm).

has significant influence on the optimal fiber angle θ . Besides, the range of the optimal fiber angles for $[\pm\theta/90_2/0]_{10s}$ thick laminated truncated conical shells are narrower than those of $[\pm\theta/90_2/0]_{2s}$ thin laminated truncated conical shells. Figs. 6–8(b) show similar trend as Figs. 3–5(b) except that the optimal fundamental frequencies ω for thick shells are higher than those of thin shells.

Fig. 9 ($r_2/r_1 = 0.6$) and Fig. 10 ($r_2/r_1 = 1$) show the typical fundamental vibration modes for both thin and thick ($[\pm\theta/90_2/0]_{2s}$ and $[\pm\theta/90_2/0]_{10s}$) shells with two fixed ends and under the optimal fiber orientation. We can find that when the L/r_1 ratio or the shell thickness increase, the vibration modes of these laminated truncated conical shells have less waves in the circumferential direction. However, when the r_2/r_1 ratio increases (i.e., approach cylindrical shell configuration), the vibration modes of the shells may have more waves in the circumferential direction. Similar results are also obtained for shells with other boundary conditions [23].

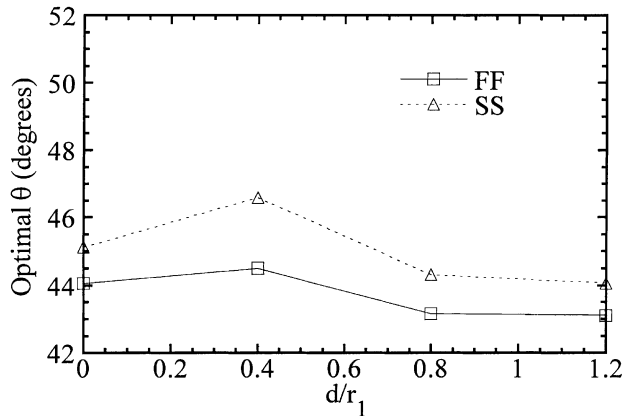
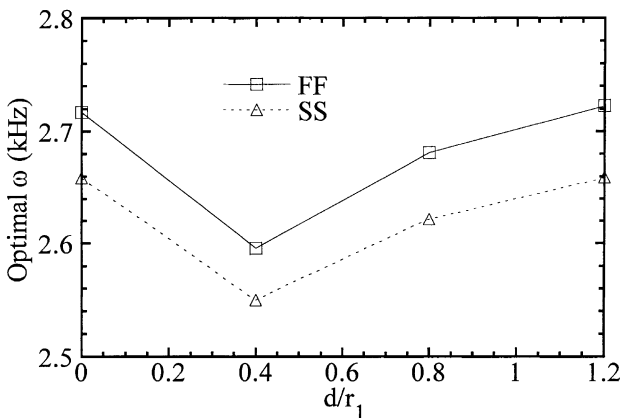
(a) Optimal fiber angle θ vs. d/r_1 ratio(b) Optimal fundamental frequency ω vs. d/r_1 ratio

Fig. 12. Effect of boundary conditions and d/r_1 ratio on optimal fiber angle and optimal fundamental frequency of $[\pm\theta/90_2/0]_{10s}$ laminated truncated conical shells with central circular cutouts ($r_1 = 10$ cm, $r_2 = 6$ cm, $L = 30$ cm).

5.2. Laminated truncated conical shells with various central circular cutouts and boundary conditions

In this section, laminated truncated conical shells with $r_1 = 10$ cm, $r_2 = 6$ cm ($r_2/r_1 = 0.6$) and $L = 30$ cm ($L/r_1 = 3$) are analyzed. These shells contain central circular cutouts with diameter d varying between 0 and 12 cm (Fig. 2(b)). As before, two laminate layups, $[\pm\theta/90_2/0]_{2s}$ and $[\pm\theta/90_2/0]_{10s}$, are chosen for analysis. In the previous section, it is shown that the results of optimization are not sensitive to the boundary conditions. Hence, in this section, only two types of boundary conditions, FF and SS, are selected for analysis.

Fig. 11 shows the optimal fiber angle θ and the associated optimal fundamental frequency ω with respect to the ratio d/r for thin ($[\pm\theta/90_2/0]_{2s}$) laminated truncated conical shells. From Fig. 11(a) we can see that the optimal fiber angles θ seem to be second-order polynomials of d/r_1 ratio. Under the same d/r_1 ratio, the optimal fiber angles of the SS shells are usually greater than those of the FF shells. Fig. 11(b) shows that under

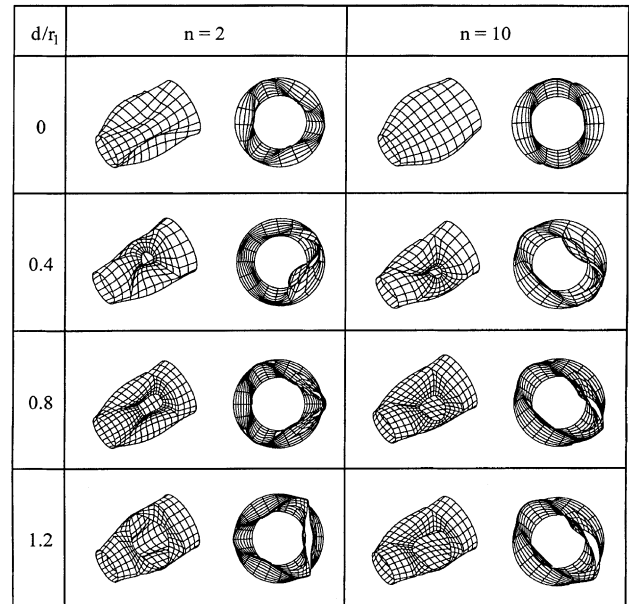
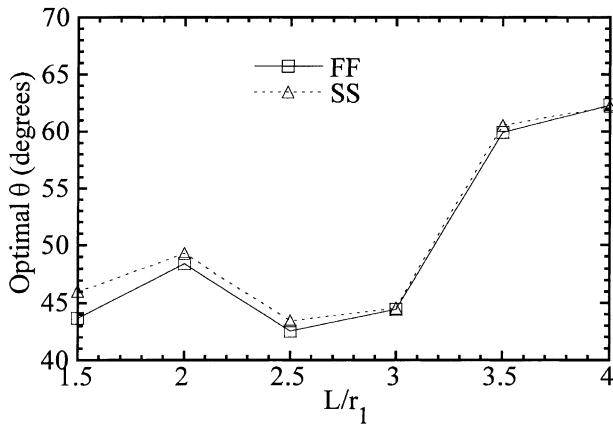


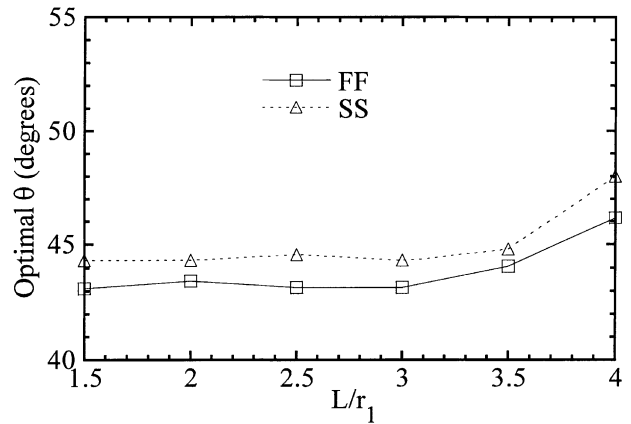
Fig. 13. Fundamental vibration mode of $[\pm\theta/90_2/0]_{ns}$ laminated truncated conical shells with central circular cutouts, with two fixed ends and under optimal fiber angles ($r_1 = 10$ cm, $r_2 = 6$ cm, $L = 30$ cm).

the same d/r_1 ratio, the optimal fundamental frequencies of FF shell are higher than those of SS shells. When the d/r_1 ratio is less than 0.4, the optimal fundamental frequencies of these shells decrease with the increase of the cutout size. However, when the d/r_1 ratio is greater than 0.4, the optimal fundamental frequencies increase with the increasing of the cutout size. The phenomenon that the fundamental frequencies increase with the increasing of the cutout size might seem strange. However, previous research did show that introducing a hole into a composite structure does not always reduce the fundamental natural frequency and, in some instances, may increase its fundamental natural frequency [24–28]. This is because that the fundamental natural frequency of an ordinary composite structure is not only influenced by cutout, but also influenced by material orthotropy, boundary condition, structural geometry, and their interactions. Fig. 12 shows the optimal fiber angle θ and the associated optimal fundamental frequency ω with respect to the ratio d/r_1 for thick ($[\pm\theta/90_2/0]_{10s}$) laminated truncated conical shells. Generally, Fig. 12(a) shows the similar trend as Fig. 11(a) except that the range of the optimal fiber angles for $[\pm\theta/90_2/0]_{10s}$ thick shells are narrower than those of $[\pm\theta/90_2/0]_{2s}$ thin shells. Fig. 12(b) also shows similar trend as Fig. 11(b). However, the influence of boundary condition is more prominent when the shell thickness becomes large.

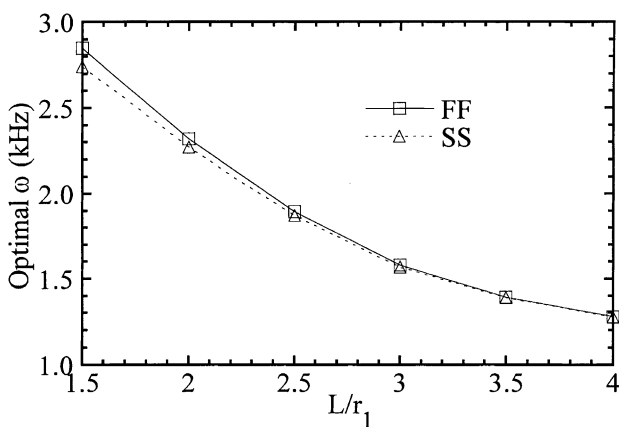
Typical fundamental vibration modes for both thin and thick ($[\pm\theta/90_2/0]_{2s}$ and $[\pm\theta/90_2/0]_{10s}$) laminated truncated conical shells with central circular cutouts, with two fixed ends and under the optimal fiber orientation are given in Fig. 13. It shows that when the cutout



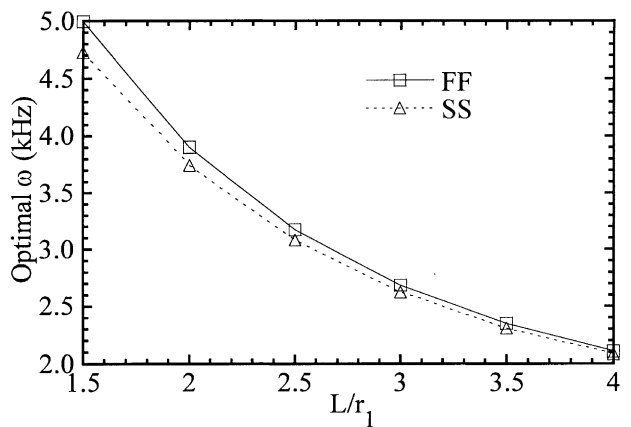
(a) Optimal fiber angle θ vs. L/r_1 ratio



(a) Optimal fiber angle θ vs. L/r_1 ratio



(b) Optimal fundamental frequency ω vs. L/r_1 ratio



(b) Optimal fundamental frequency ω vs. L/r_1 ratio

Fig. 14. Effect of boundary conditions and L/r_1 ratio on optimal fiber angle and optimal fundamental frequency of $[\pm\theta/90_2/0]_{2s}$ laminated truncated conical shells with a central circular cutout ($r_1 = 10$ cm, $r_2 = 6$ cm, $d = 8$ cm).

Fig. 15. Effect of boundary conditions and L/r_1 ratio on optimal fiber angle and optimal fundamental frequency of $[\pm\theta/90_2/0]_{10s}$ laminated truncated conical shells with a central circular cutout ($r_1 = 10$ cm, $r_2 = 6$ cm, $d = 8$ cm).

sizes are large, the fundamental vibration modes of the shells tend to have more distortion around the hole. Similar results are also obtained for shells with other boundary conditions [23].

5.3. Laminated truncated conical shells containing central circular cutouts with various lengths and boundary conditions

In this section, laminated truncated conical shells with $r_1 = 10$ cm and $r_2 = 6$ cm are analyzed. The length of the shell, L , varies between 15 and 40 cm. These shells contain central circular cutouts with diameter $d = 8$ cm (Fig. 2(b)). As before, two types of boundary conditions, FF and SS, and two laminate layups, $[\pm\theta/90_2/0]_{2s}$ and $[\pm\theta/90_2/0]_{10s}$, are selected for analysis.

Figs. 14 and 15 show the optimal fiber angle θ and the associated optimal fundamental frequency ω with respect to the L/r_1 ratio for thin and thick ($[\pm\theta/90_2/0]_{2s}$ and $[\pm\theta/90_2/0]_{10s}$) laminated truncated conical shells

with central circular cutouts. For thin shells, it seems that the optimal fiber angles θ seem to be fourth-order polynomials of L/r_1 ratio (Fig. 14(a)). For thick shells, when L/r_1 ratio is small (say $L/r_1 \leq 3$), the optimal fiber angles seem to approach constant values (Fig. 15(a)). Comparing Figs. 14 and 15(a) with Figs. 3 and 6(a), we can see that the cutouts do have influence on the optimal fiber angles of laminated truncated conical shells. This influence is more significant for thin shells than that for thick shells. From Figs. 14 and 15(b) we can see that for both thin and thick shells containing central circular cutout, their optimal fundamental frequencies decrease with the increase of L/r_1 ratio. Again, the optimal fundamental frequencies seem not to be sensitive to the boundary conditions, especially when the L/r_1 ratio becomes large.

Typical fundamental vibration modes for both thin and thick ($[\pm\theta/90_2/0]_{2s}$ and $[\pm\theta/90_2/0]_{10s}$) truncated conical shells containing central circular cutouts with two fixed ends and under optimal fiber orientations are

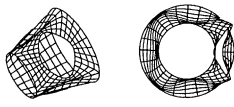
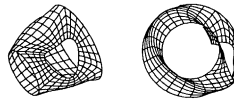
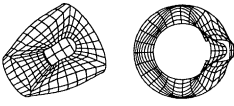
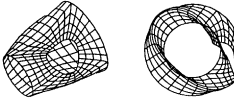
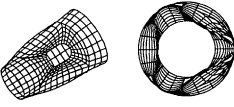
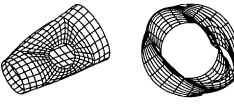
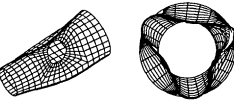
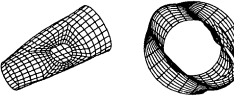
L/r_1	$n=2$	$n=10$
1.5		
2		
3		
4		

Fig. 16. Fundamental vibration mode of $[\pm\theta/90_2/0]_{ns}$ laminated truncated conical shells with central circular cutouts, with two fixed ends and under optimal fiber angles ($r_1 = 10$ cm, $r_2 = 6$ cm, $d = 8$ cm).

given in Fig. 16. Comparing Fig. 16 with Fig. 9, we can observe that the cutouts cause the fundamental vibration modes of shells to have significant distortion around the hole area. This distortion is more significant for thick shells than that for thin shells. When the L/r_1 ratios are large, the fundamental vibration modes of shells seem to be less sensitive to the present of cutouts. Similar results are also obtained for laminated truncated conical shells with other boundary conditions [23].

6. Conclusions

For the optimal free vibration analysis of $[\pm\theta/90_2/0]_{2s}$ and $[\pm\theta/90_2/0]_{10s}$ laminated truncated conical shells with various shell lengths, radius ratios, circular cutouts and boundary conditions, the following conclusions may be drawn:

1. The results of optimization of laminated truncated conical shells are not sensitive to the boundary conditions but are sensitive to the shell thickness and central circular cutout.
2. The range of the optimal fiber angles θ decrease with the increasing of the r_2/r_1 ratio. In addition, the range of the optimal fiber angles for thick laminated truncated conical shells are narrower than those of thin shells.
3. The optimal fundamental frequency ω generally decreases with the increasing of L/r_1 ratio and the decreasing of shell thickness. In addition, the optimal fundamental frequency ω is not influenced by the r_2/r_1 ratio significantly.

4. The optimal fundamental frequencies of laminated truncated conical shells may not decrease with the increase of the cutout size.
5. When the L/r_1 ratio or the shell thickness increase, the vibration modes of the laminated truncated conical shells have less waves in the circumferential direction. However, when the r_2/r_1 ratio increases, the vibration modes of the shells may have more waves in the circumferential direction.
6. The cutouts cause the fundamental vibration modes of truncated conical shells to have significant distortion around the hole area, specially when the cutout size is large. This distortion is more prominent for thick shells than that for thin shells. When the L/r_1 ratio is large, the fundamental vibration modes of shells seem to be less sensitive to the present of cutouts.

Acknowledgements

This work was financially supported by the National Science Council of the Republic of China under grant NSC89-2211-E006-136.

References

- [1] Leissa AW. Recent studies in plate vibrations: 1981–85, Part II, complicating effects. *Shock Vib Dig* 1987;19:10–24.
- [2] Wilkins DJ, Bert CW, Egle DM. Free vibrations of orthotropic sandwich conical shells with various boundary conditions. *J Sound Vib* 1970;13(2):211–28.
- [3] Sheinman I, Greif S. Dynamic analysis of laminated shells of revolution. *J Compos Mater* 1984;18:200–15.
- [4] Sankaranarayanan N, Chandrasekaran K, Ramaiyan G. Free vibrations of laminated conical shells of variable thickness. *J Sound Vib* 1988;123(2):357–71.
- [5] Kayan A, Vinson JR. Free vibration analysis of laminated composite truncated circular conical shells. *AIAA J* 1990;28(7):1259–69.
- [6] Tong L. Free vibration of laminated conical shells including transverse shear deformation. *Int J Solids Struct* 1994;31(4):443–56.
- [7] Khatri KN. Vibrations of arbitrarily laminated fiber reinforced composite material truncated conical shell. *J Reinf Plast Compos* 1995;14:923–48.
- [8] Sivadas KR. Vibration analysis of pre-stressed thick circular conical composite shells. *J Sound Vib* 1995;186(1):87–97.
- [9] Lim CW, Liew K, Kitipornchai M. Vibration of cantilevered laminated composite shallow conical shells. *Int J Solids Struct* 1998;35(15):1695–707.
- [10] Korjakin A, Rikards R, Chate A, Altenbach H. Analysis of free damped vibrations of laminated composite conical shells. *Compos Struct* 1998;41(15):39–47.
- [11] Bert CW. Literature review – Research on dynamic behavior of composite and sandwich plates – V: Part II. *Shock Vib Dig* 1991;23:9–21.
- [12] Raouf RA. Tailoring the dynamic characteristics of composite panels using fiber orientation. *Compos Struct* 1994;29:259–67.
- [13] Abrate S. Optimal design of laminated plates and shells. *Compos Struct* 1994;29:269–86.
- [14] Schmit LA. Structural synthesis – its genesis and development. *AIAA J* 1981;19(10):1249–63.

- [15] Zienkiewicz OC, Champbell, JS. Shape optimization and sequential linear programming. In: Gallagher RH, Zienkiewicz OC, editors. *Optimum structural design, theory and applications*. New York: Wiley; 1973. p. 109–26.
- [16] Vanderplaats GN. *Numerical optimization techniques for engineering design with applications*. New York: McGraw-Hill; 1984 [chapter 2].
- [17] Hibbitt, Karlsson & Sorensen, Inc. *ABAQUS user, theory and verification manuals*. Version 5.8, Providence, Rhode Island, 1999.
- [18] Whitney JM. Shear correction factors for orthotropic laminates under static load. *J Appl Mech* 1973;40:302–4.
- [19] Cook RD, Malkus DS, Plesha ME. *Concepts and applications of finite element analysis*, 3rd ed. New York: Wiley; 1989 [chapter 13].
- [20] Bathe KJ, Wilson EL. Large eigenvalue problems in dynamic analysis. *J Eng Mech Division, ASCE* 1972;98:1471–85.
- [21] Kolman B, Beck RE. *Elementary linear programming with applications*. Orlando: Academic Press; 1980 [chapter 2].
- [22] Crawley EF. The natural modes of graphite/epoxy cantilever plates and shells. *J Compos Mater* 1979;13:195–205.
- [23] Ou S-C. Influence of geometry and boundary conditions on optimal fundamental frequencies and associated optimal fiber angles of symmetrically laminated truncated conical shells. M.S. Thesis, Department of Civil Engineering, National Cheng Kung University, Tainan, Taiwan, ROC, 1999.
- [24] Hu H-T, Ho M-H. Influence of geometry and end conditions on optimal fundamental natural frequencies of symmetrically laminated plates. *J Reinf Plast Compos* 1996;15(9):877–93.
- [25] Hu H-T, Juang C-D. Maximization of the fundamental frequencies of laminated curved panels against fiber orientation. *J Aircr* 1997;34(6):792–801.
- [26] Hu H-T, Tsai C-Y. Maximization of the fundamental frequencies of laminated cylindrical shells with respect to fiber orientations. *J Sound Vib* 1999;225(4):723–40.
- [27] Lee HP, Lim SP, Chow ST. Free vibration of composite rectangular plates with rectangular cutouts. *Compos Struct* 1987;8:63–81.
- [28] Ramakrishna S, Rao SKM, Rao NS. Free vibration analysis of laminates with circular cutout by hybrid-stress finite element. *Compos Struct* 1992;21:177–85.